Comparative Experimental Study of Fixed Temperature and Fixed Heat Flux Boundary Conditions in Turbulent Thermal Convection

Shi-Di Huang (黄仕迪),[1] Fei Wang (王飞),[1] Heng-Dong Xi (郗恒东),[2] and Ke-Qing Xia (夏克青)[1]
[1]Department of Physics, The Chinese University of Hong Kong, Shatin, Hong Kong, China
[2]School of Aeronautics, Northwestern Polytechnical University, Xi'an, China

(Received 24 February 2015; revised manuscript received 11 August 2015; published 5 October 2015)

We report the first experimental study of the influences of the thermal boundary condition on turbulent thermal convection. Two configurations were examined: one had a constant heat flux at the bottom boundary and a constant temperature at the top (CFCT cell); the other had constant temperatures at both boundaries (CTCT cell). In addition to producing different temperature stability in the boundary layers, the differences in the boundary condition lead to rather unexpected changes in the flow dynamics. It is found that, surprisingly, reversals of the large-scale circulation occur more frequently in the CTCT cell than in the CFCT cell, despite the fact that in the former its flow strength is on average 9% larger than that in the latter. Our results not only show which aspects of the thermal boundary condition are important in thermal turbulence, but also reveal that, counterintuitively, the stability of the flow is not directly coupled to its strength.

DOI: 10.1103/PhysRevLett.115.154502 PACS numbers: 47.55.pb, 44.20.+b, 47.27.-i

The importance of the boundary condition (BC) in fluid mechanics has long been recognized. For instance, slip and nonslip BCs are totally different in controlling the flow dynamics [1,2]. In thermal turbulence, the thermal boundary condition is important in a similar way. However, compared to the comprehensive knowledge of velocity BC [3–5], our understanding of thermal BC, especially its impact on turbulent convection, is far from complete. The two most general thermal BCs are fixed heat flux and fixed temperature. How the two different BCs will affect the flow dynamics and transport properties in convective turbulence is not only of fundamental interest, but is also crucial for understanding the convection phenomena occurring ubiquitously in nature (see, e.g., Refs. [6–8] and references therein). An idealized model for studying thermal turbulence is the turbulent Rayleigh-Bénard (RB) convection, a fluid layer heated from below and cooled from the top [9–12]. Despite its great importance, there are just a few numerical and theoretical studies so far on the effects of thermal BC in turbulent RB flow [13–16]. These studies mostly focused on the heat transport behavior and the main results are that fixed temperature and fixed flux BCs lead to an essentially the same response in the Nusselt number (the dimensionless heat flux) [14,15]. Another key quantity for characterizing RB flow is the Reynolds number Re (nondimensional flow strength), which is associated with the dynamics of the large-scale circulation (LSC) surviving in the turbulent background [9]. However, how the thermal boundary condition will alter the dynamical features of the LSC has received little attention. The only attempt so far is from a two-dimensional simulation, in which the authors noted similarities between the large-scale dynamics for fixed temperature and fixed flux conditions, but no systematic comparison has been made [14]. The incomplete understanding of the roles of the thermal boundary condition in turbulent convection and the absence of experimental study on this issue motivate the present work.

In this Letter we report a novel experimental study of the influences of the thermal boundary condition on turbulent convection, with special focus on its effects on the flow dynamics. To the best of our knowledge, our work is the first systematic study of the importance of the thermal boundary condition on the flow dynamics in thermal turbulence. Two types of convection cells were used in the experiment, which differed only in how the bottom plate was heated but were otherwise identical. Briefly, the cells were of rectangular shape with copper top and bottom plates and a Plexiglas sidewall, as described in Ref. [17]. The first type has a resistive film heater attached to the bottom plate with constant power input and a temperature-regulated circulator keeping the top plate at constant temperature. Clearly, the nominal thermal BCs for this type of cell are constant heat flux at the bottom plate and constant temperature at the top (henceforth referred to as the CFCT cell). The second type has its bottom plate heated by another circulator so that the temperatures of both plates were regulated by circulators separately and both were nominally under constant temperature thermal BC. We call this one the CTCT cell hereafter. It should be noted that the condition of fixed temperature (heat flux) holds only approximately here, because a temporally and spatially varying temperature (heat flux) within the plates is inevitable for laboratory experiments owing to the finite conductivity effect of the plates [18,19]. Both cells have a dimension of 12.6 cm (high) $\times$ 12.6 cm (long) $\times$ 3.8 cm (wide). In order to extend the parameter range,

another set of larger cells with all dimensions twice as large as the smaller ones were used. Therefore, a total of four convection cells were used in the present study: two each with the CFCT configuration and two each with the CTCT one. The combined range of the Rayleigh number $\mathrm{Ra} = \alpha g \Delta T H^3/\nu\kappa$ spans from 8.7×10^7 to 1.5×10^{10}. Here, ΔT is the temperature difference across the fluid layer with the height being H, g is the gravitational acceleration, and α, ν, and κ are the thermal expansion coefficient, kinematic viscosity, and thermal diffusivity of water, respectively.

We first examine the differences in boundary stability between the two configurations. The top panel of Fig. 1 shows examples of temperature fluctuation time series inside the conducting plates at $\mathrm{Ra} = 1 \times 10^9$ for the CFCT and CTCT configurations from the small cells, respectively. It is seen that, for the CFCT cell, the fluctuations inside the bottom plate are distinctly larger than those inside the top plate, whereas for the CTCT cell, the data from different plates collapse well with each other. In fact, for the three plates whose temperatures were regulated by circulators, they yield approximately the same form in probability density functions (PDF) and thus the same standard deviation [Fig. 1(c)]. This phenomenon is found to be true for all values of Ra covered in the study. As seen from Fig. 1(d), the three plates under fixed temperature from the small cells have almost the same standard deviations that are much smaller than those for the plate

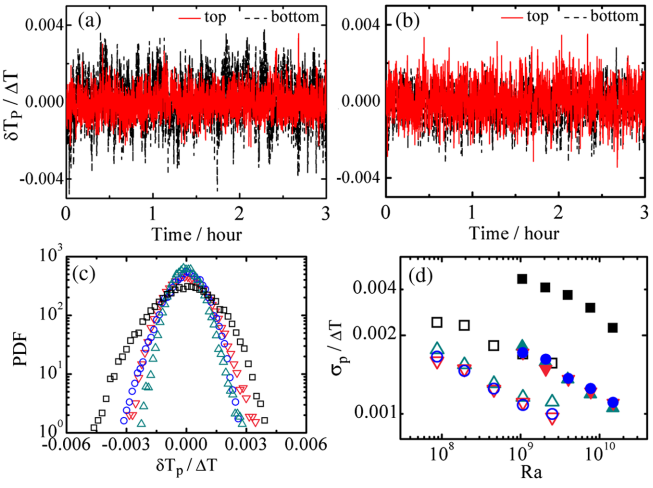

FIG. 1 (color online). Top panel: Time series of normalized temperature fluctuations inside the top and bottom plates at $\mathrm{Ra} = 1 \times 10^9$ for the CFCT (a) and CTCT (b) cells, respectively. (c) The corresponding PDFs for the data in (a) and (b). (d) The Ra dependence of the normalized temperature standard deviation inside the conducting plates for all the cells. The solid and open symbols are for the data in the large and small cells, respectively. The square and upward-pointing triangle represent the data from the bottom and top plates of the CFCT cells, while the downward-pointing triangle and circle represent the data from the bottom and top plates of the CTCT cells.

under fixed flux, and the same is true for the large cells [20]. This indicates that the CTCT cell has a better stability in boundary temperature and a higher top-bottom symmetry than the CFCT cell, the significance of which has not been recognized before.

In RB convection, thermal boundary layers (BL) will adjust their thicknesses by emitting plumes to remain marginally stable [21]. Thus, the stability of thermal BLs should be different for fixed temperature and fixed flux boundary conditions, as these BCs will exert different controls on the boundary layers. Figure 2 shows the profiles of the temperature standard deviation in the CFCT and CTCT cells for $\mathrm{Ra} = 1 \times 10^9$, which were measured by traversing a small thermistor vertically from the bottom plate along the central axis of the cell [22]. It is seen clearly that, inside the boundary layer, the temperature fluctuations are smaller in the CTCT cell (fixed temperature) than in the CFCT cell (fixed heat flux). These results are consistent with previous numerical studies [13,15].

As plume emissions are manifestations of the BL instability and the LSC is essentially an organized motion of thermal plumes [23], the changes in the thermal BLs should be reflected in the plume dynamics and thus in the properties of the LSC. To find out how the LSC is affected under the two configurations, we first investigate the strength of the LSC based on the temperature signals from the opposite conducting plates. By analyzing their cross-correlation function, the velocity of the LSC, and thus the corresponding Re number, are obtained [24]. It is seen in Fig. 3 that the Re in the two CTCT cells are on average ~9% larger than those in the CFCT cells, indicating that the LSC is stronger in the CTCT configuration. To obtain a global picture of the flow field, we conducted particle image velocimetry (PIV) measurement [17]. Figure 4 shows the mean velocity field measured at $\mathrm{Ra} = 1 \times 10^9$, by averaging 7000 vector maps acquired at ~2 Hz for the CFCT and CTCT cells, respectively. As indicated by the scale bar, the maximum velocity in the

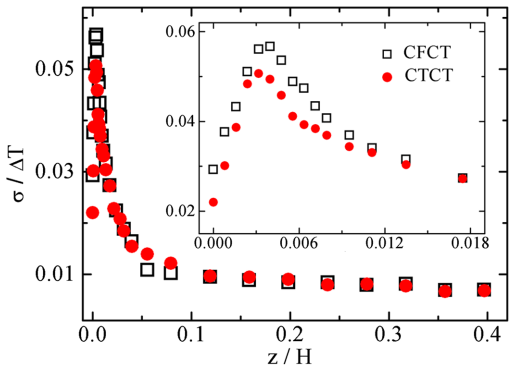

FIG. 2 (color online). Normalized temperature standard deviation vs normalized vertical distance from the bottom plate measured in the CFCT and CTCT cells ($\mathrm{Ra} = 1 \times 10^9$). The inset shows an enlarged portion near the boundary.

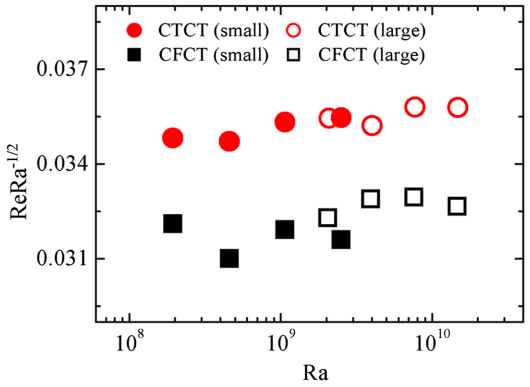

FIG. 3 (color online). The compensated Reynolds number as a function of Ra measured in different cells.

CTCT cell is about 8% larger than that in the CFCT cell, which agrees excellently with the Re data. Moreover, the increase in flow strength is not limited to the maximum velocity, but is true for the overall flow: the stronger large-scale flow stirs the bulk fluid more forcefully so that the "quiescent" core region becomes smaller in the CTCT cell. It is known that in RB convection the turbulent energy is provided by thermal plumes [17]. Therefore, this finding is consistent with the results from previous numerical studies

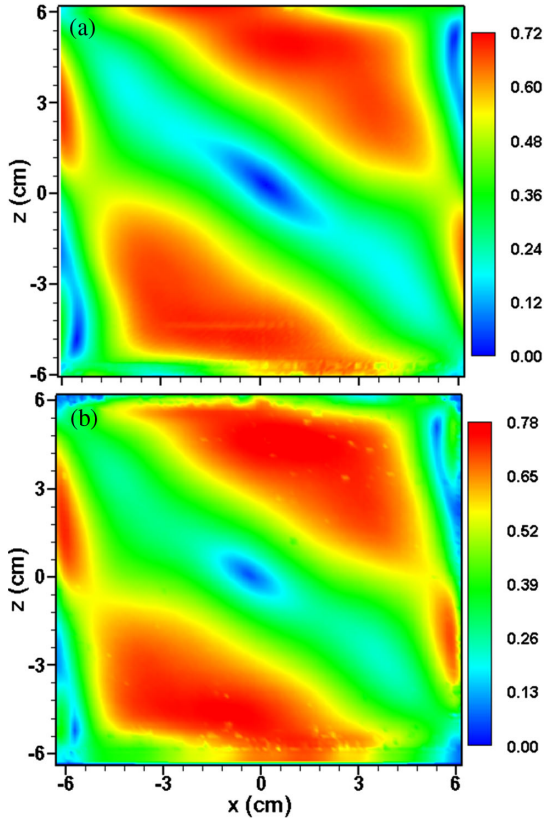

FIG. 4 (color online). Color-coded contour maps of mean velocity field measured in the CFCT (a) and CTCT (b) cells for $\mathrm{Ra} = 1 \times 10^9$. The scale bar represents $(U^2 + W^2)^{1/2}$ in units of cm/s.

that plume emissions are stronger for constant temperature than for constant heat flux [13,25].

One would ordinarily think that, coexisting with the turbulent background of the RB system, a stronger LSC would be more able to keep its momentum and thus the flow direction. However, we find this not to be the case regarding its reversal behavior. Here, reversals refer to a phenomenon that the LSC suddenly reverses its flow direction in an erratic manner, which is one of the intriguing features of the LSC [5,26–29]. In the present rectangular geometry, the hot rising and cold falling plumes will switch between the left and right sides of the convection cell when the LSC changes from one circulating direction to the other. Therefore, the temperature contrast $\delta = T_{\mathrm{right}} - T_{\mathrm{left}}$ will change its sign during a reversal event and thus is a good indicator of reversals [29], where T_{right} and T_{left} are the temperatures measured by the thermistors imbedded in the right and left sides of the plate. To discuss the reversal frequency quantitatively, we first define the start and end times of one reversal event when δ changes its sign, from which we obtain the time interval between two successive reversals [30]. The reversal frequency is then calculated by taking the inverse of the mean time interval of successive reversals. In order to obtain good statistics, the measurement was made in the two small cells only, where there are much more reversals. The obtained Ra dependence of the reversal frequencies f_{CTCT} and f_{CFCT} are plotted in Fig. 5. It is seen that the reversal frequencies in both cases decrease with increasing Ra, which is consistent with earlier findings in this system [29,30]. What is surprising here is that the LSC reverses its direction more frequently in the CTCT cell than in the CFCT cell, despite the fact that in the former the LSC is stronger and the temperature fluctuations in its BL are smaller. Moreover, this trend becomes more so with increasing Ra, as shown in the inset of Fig. 5. Interestingly, a decoupling of the flow strength and its stability of circulating states, i.e., the reversal behavior, are also found

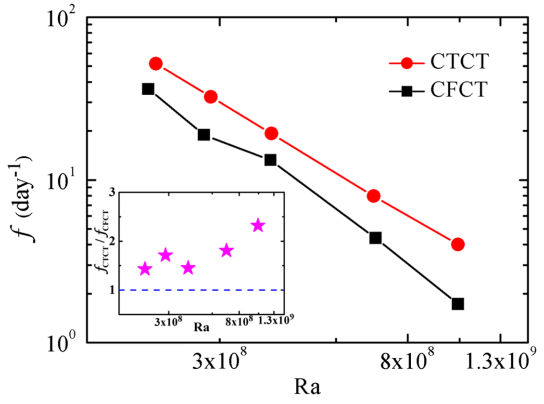

FIG. 5 (color online). Ra dependence of the reversal frequency f. The solid lines are drawn to guide the eyes. Inset: The ratio of $f_{\mathrm{CTCT}}/f_{\mathrm{CFCT}}$.

in the studies of other turbulent flows [8,31]. In fact, reversal phenomena are quite general that they have been observed in a wide variety of fluid flows [31–33] and share some common features with the LSC reversal in the RB convection. Although, the various systems are different in nature, their reversal behavior may be underpinned by the same principle. For example, it has been suggested that fixed heat flux BC, rather than the fixed temperature BC that has been widely used in Geodynamo models, is a more natural choice for the earth system and the two BCs may yield different reversal frequency of the geomagnetic field [7]. Therefore, the present finding that the LSC reversal frequency has a sensitive dependence on the thermal boundary condition may bring important insights into the general phenomenon of flow reversals.

In summary, we have experimentally shown for the first time that, in addition to producing different temperature stability in the boundary layers, the fixed temperature and fixed heat flux boundary conditions in turbulent thermal convection can give rise to rather unexpected changes in the flow dynamics. It is found that both the flow strength and the reversal frequency of the LSC under the fixed temperature boundary condition are higher than they are in the fixed heat flux case. These differences in the bulk flow dynamics could arise from changes in boundary layer instabilities associated with the two types of thermal boundary conditions. Our results not only show clearly in what aspects the thermal BC is important in turbulent convective flows, but also reveal that the stability of the flow is not directly coupled to its strength. One way to understand this counterintuitive phenomenon is to note that the buildup of a large-scale flow circulating in a particular direction actually breaks down the symmetry of the system. Thus, reversals of the LSC can be viewed as a process for the system to restore its symmetry in a statistical way. In other words, the statistical properties of flow reversals may depend on the symmetry of the system and how it is broken. In the present study, because the CTCT cell has a more symmetric boundary condition than the CFCT cell does, so more reversals are "required" to recover its symmetry. To substantiate this argument, further studies, both experimental and theoretical, are required. We remark that such a symmetry-restoring mechanism has also been proposed recently to understand the geomagnetic reversals [32]. As the phenomena of flow reversals occur in a wide variety of fluid flows, the idea that flow reversal is a symmetry restoration process should stimulate further studies.

We thank Chao Sun for helpful discussions and suggestions on the manuscript. This work was supported by the Research Grants Council of Hong Kong SAR under Grants No. CUHK403712 and No. CUHK404513. H. D. X. acknowledges support from The National Science Foundation of China through Grant No. 11472094 and the Fundamental Research Funds for the Central Universities of China.

[1] S. Richardson, On the no-slip boundary condition, J. Fluid Mech. **59**, 707 (1973).
[2] P. A. Thompson and S. M. Troian, A general boundary condition for liquid flow at solid surfaces, Nature (London) **389**, 360 (1997).
[3] J.-Q. Zhong and J. Zhang, Thermal convection with a freely moving top boundary, Phys. Fluids **17**, 115105 (2005).
[4] E. P. van der Poel, R. Ostilla-Mónico, R. Verzicco, and D. Lohse, Effect of velocity boundary conditions on the heat transfer and flow topology in two-dimensional Rayleigh-Bénard convection, Phys. Rev. E **90**, 013017 (2014).
[5] M. K. Verma, S. C. Ambhire, and A. Pandey, Flow reversals in turbulent convection with free-slip walls, Phys. Fluids **27**, 047102 (2015).
[6] C. Grigné, S. Labrosse, and P. J. Tackley, Convection under a lid of finite conductivity: Heat flux scaling and application to continents, J. Geophys. Res. **112**, B08402 (2007).
[7] A. Sakuraba and P. H. Roberts, Generation of a strong magnetic field using uniform heat flux at the surface of the core, Nat. Geosci. **2**, 802 (2009).
[8] A. J. Biggin, B. Steinberger, J. Aubert, N. Suttie, R. Holme, T. Torsvik, D. G. van der Meer, and D. J. J. van Hinsbergen, Possible links between long-term geomagnetic variations and whole-mantle convection processes, Nat. Geosci. **5**, 526 (2012).
[9] G. Ahlers, S. Grossmann, and D. Lohse, Heat transfer and large scale dynamics in turbulent Rayleigh-Bénard convection, Rev. Mod. Phys. **81**, 503 (2009).
[10] D. Lohse and K.-Q. Xia, Small scale properties of turbulent Rayleigh-Bénard convection, Annu. Rev. Fluid Mech. **42**, 335 (2010).
[11] F. Chillà and J. Schumacher, New perspectives in turbulent Rayleigh-Bénard convection, Eur. Phys. J. E **35**, 58 (2012).
[12] K.-Q. Xia, Current trends and future directions in turbulent thermal convection, Theor. Appl. Mech. Lett. **3**, 052001 (2013).
[13] R. Verzicco and K. R. Sreenivasan, A comparison of turbulent thermal convection between conditions of constant temperature and constant heat flux, J. Fluid Mech. **595**, 203 (2008).
[14] H. Johnston and C. R. Doering, Comparison of turbulent thermal convection between conditions of constant temperature and constant flux, Phys. Rev. Lett. **102**, 064501 (2009).
[15] R. J. Stevens, D. Lohse, and R. Verzicco, Prandtl and Rayleigh number dependence of heat transport in high Rayleigh number thermal convection, J. Fluid Mech. **688**, 31 (2011).
[16] T. Weidauer and J. Schumacher, Moist turbulent Rayleigh-Bénard convection with Neumann and Dirichlet boundary conditions, Phys. Fluids **24**, 076604 (2012).
[17] K.-Q. Xia, C. Sun, and S.-Q. Zhou, Particle image velocimetry measurement of the velocity field in turbulent thermal convection, Phys. Rev. E **68**, 066303 (2003).
[18] F. Chillà, M. Rastello, S. Chaumat, and B. Castaing, Ultimate regime in Rayleigh–Bénard convection: The role of plates, Phys. Fluids **16**, 2452 (2004).
[19] R. Verzicco, Effects of nonperfect thermal sources in turbulent thermal convection, Phys. Fluids **16**, 1965 (2004).

[20] Note that the data from the large cells are systematically larger than those from the small cells. Such an interesting observation of size-dependent flow properties and the reasons for it are beyond the scope of this Letter but will be discussed in detail elsewhere. The collapse of the data from the bottom plate of the CFCT small cell and the data from the three plates of the large cells under fixed temperature boundary condition is believed to be a coincidence.

[21] W. V. R. Malkus, The heat transport and spectrum of thermal turbulence, Proc. R. Soc. A **225**, 196 (1954).

[22] S.-L. Lui and K.-Q. Xia, Spatial structure of the thermal boundary layer in turbulent convection, Phys. Rev. E **57**, 5494 (1998).

[23] H.-D. Xi, S. Lam, and K.-Q. Xia, From laminar plumes to organized flows: the onset of large-scale circulation in turbulent thermal convection, J. Fluid Mech. **503**, 47 (2004).

[24] E. Brown, D. Funfschilling, and G. Ahlers, Anomalous Reynolds-number scaling in turbulent Rayleigh-Bénard convection, J. Stat. Mech. (2007) P10005.

[25] J. C. R. Hunt, A. J. Vrieling, F. T. M. Nieuwstadt, and H. J. S. Fernando, The influence of the thermal diffusivity of the lower boundary on eddy motion in convection, J. Fluid Mech. **491**, 183 (2003).

[26] K. R. Sreenivasan, A. Bershadskii, and J. J. Niemela, Mean wind and its reversal in thermal convection, Phys. Rev. E **65**, 056306 (2002).

[27] E. Brown, A. Nikolaenko, and G. Ahlers, Reorientation of the Large-Scale Circulation in Turbulent Rayleigh-Bénard Convection, Phys. Rev. Lett. **95**, 084503 (2005).

[28] H.-D. Xi and K.-Q. Xia, Cessations and reversals of the large-scale circulation in turbulent thermal convection, Phys. Rev. E **75**, 066307 (2007).

[29] K. Sugiyama, R. Ni, R. J. A. M. Stevens, T. S. Chan, S.-Q. Zhou, H.-D. Xi, C. Sun, S. Grossmann, K.-Q. Xia, and D. Lohse, Flow Reversals in Thermally Driven Turbulence, Phys. Rev. Lett. **105**, 034503 (2010).

[30] R. Ni, S.-D. Huang, and K.-Q. Xia, Reversals of the large-scale circulation in quasi-2D Rayleigh-Bénard convection, J. Fluid Mech. **778**, R5 (2015).

[31] F. Pétrélis and S. Fauve, Chaotic dynamics of the magnetic field generated by dynamo action in a turbulent flow, J. Phys. Condens. Matter **20**, 494203 (2008).

[32] B. Gallet, J. Herault, C. Laroche, F. Pétrélis, and S. Fauve, Reversals of a large-scale field generated over a turbulent background, Geophys. Astrophys. Fluid Dyn. **106**, 468 (2012).

[33] P. K. Mishra, J. Herault, S. Fauve, and M. K. Verma, Dynamics of reversals and condensates in two-dimensional Kolmogorov flows, Phys. Rev. E **91**, 053005 (2015).